



1 An Arctic watershed observatory at Lake Peters,  
2 Alaska: weather-glacier-river-lake system data for  
3 2015-2018

4

5 **Authors**

6 Ellie Broadman<sup>1</sup>, Lorna L. Thurston<sup>2</sup>, Nicholas P. McKay<sup>1</sup>, Darrell S. Kaufman<sup>1</sup>, Erik Schiefer<sup>1</sup>,  
7 David Fortin<sup>3</sup>, Jason Geck<sup>4</sup>, Michael G. Loso<sup>5</sup>, Matt Nolan<sup>6</sup>, Stéphanie H. Arcusa<sup>1</sup>, Christopher  
8 W. Benson<sup>1</sup>, Rebecca A. Ellerbroek<sup>1</sup>, Michael P. Erb<sup>1</sup>, Cody C. Routson<sup>1</sup>, Charlotte Wiman<sup>1</sup>, A.  
9 Jade Wong<sup>1</sup>

10 1. School of Earth and Sustainability, Northern Arizona University, Flagstaff, Arizona, 86011,  
11 USA

12 2. Stillwater Sciences, 2855 Telegraph Ave, Ste 400, Berkeley, California, 94705, USA

13 3. Department of Geography and Planning, University of Saskatchewan, Saskatoon, SK S7N  
14 5C8, Canada

15 4. Environmental Science Department, Alaska Pacific University, Anchorage, Alaska, 99508

16 5. Inventory and Monitoring Program, Wrangell-St. Elias National Park and Preserve, Copper  
17 Center, Alaska, USA

18 6. Fairbanks Fodar, Fairbanks, Alaska, USA



## 19 Abstract

20 Datasets from a four-year monitoring effort at Lake Peters, a glacier-fed lake in Arctic Alaska,  
21 are described and presented with accompanying methods, biases, and corrections. Three  
22 meteorological stations documented air temperature, relative humidity, and rainfall at different  
23 elevations in the Lake Peters watershed. Data from ablation stake stations on Chamberlin  
24 glacier were used to quantify glacial melt, and measurements from two hydrological stations  
25 were used to reconstruct continuous discharge for the two primary inflows to Lake Peters,  
26 Carnivore and Chamberlin Creeks. The lake's thermal structure was monitored using a network  
27 of temperature sensors on moorings, the lake's water level was recorded using pressure  
28 sensors, and sedimentary inputs to the lake were documented by sediment traps. We  
29 demonstrate the utility of these datasets by examining a flood event in July 2015, though other  
30 uses include studying intra- and inter-annual trends in this weather-glacier-river-lake system,  
31 contextualizing interpretations of lakes sediment cores, and providing background for modeling  
32 studies. All DOI-referenced datasets described in this manuscript are archived at the National  
33 Science Foundation Arctic Data Center at the following overview webpage for the project:  
34 <https://arcticdata.io/catalog/view/urn:uuid:517b8679-20db-4c89-a29c-6410cbd08afe> (Kaufman  
35 et al., 2019e).

## 36 1. Introduction

37 Arctic glacier-fed lakes are complex and dynamic systems that are influenced by diverse  
38 physical and biological processes. Long-term instrumental datasets that document how weather  
39 and climate impact glaciers, basin hydrology, and sediment transport through rivers and lakes  
40 are rare, especially in the Arctic. Such datasets are critical for studying how Arctic glacier-river-  
41 lake catchments operate as a system, for understanding the processes that control sediment



42 accumulation in lakes, and for contextualizing modern climatic and environmental change  
43 relative to past centuries.

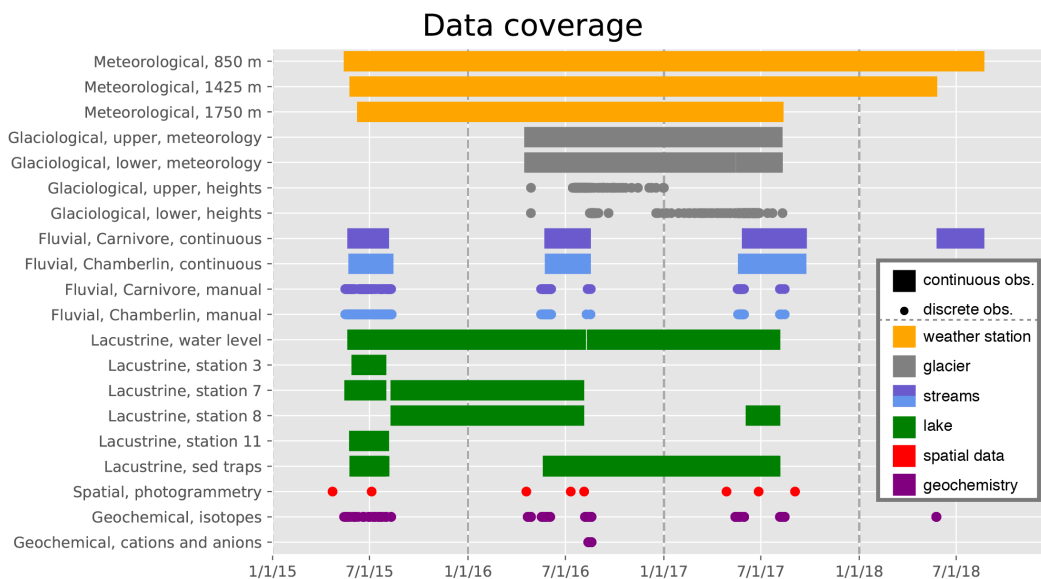
44

45 Here we present the results of a four-year instrumentation campaign in the watershed of Lake  
46 Peters, a large glacial lake located in the northeastern Brooks Range within Alaska's Arctic  
47 National Wildlife Refuge. Lake Peters is a particularly valuable site for such an observatory due  
48 to the variety of components influencing processes within the lake, including both a relatively  
49 small, glacially-dominated inflow (Chamberlin Creek) as well as a larger primary inlet with less  
50 glacier coverage (Carnivore Creek). A research station at Lake Peters was first established in  
51 the late 1950's by the Department of the Navy as a substation of the Barrow Naval Arctic  
52 Research Laboratory, and is maintained as an administrative facility by the U.S. Fish and  
53 Wildlife Service. In 2015, an array of instruments were installed and observational data  
54 collection commenced for a variety of components of the weather-glacier-river-lake system (Fig.  
55 1). All instrument installations were non-permanent in recognition of the Wilderness status of the  
56 study area.

57

58 By collecting meteorological, glaciological, fluvial, lacustrine, spatial, and geochemical data  
59 within the Lake Peters catchment, interconnections in the local hydrologic system can be  
60 quantified and explored in detail. Additionally, this multi-year monitoring study provides useful  
61 context for the interpretation of past lake sediments from Lake Peters (Benson, 2018; Benson et  
62 al., in review). In the interest of making these unique and valuable data readily accessible to  
63 potential users, the objective of this manuscript is to document and describe the datasets, as  
64 well as data collection methods, biases, and corrections.

65



66

67 Figure 1. Temporal coverage of data collected in the Lake Peters catchment. Data are either  
 68 continuous hourly or bi-hourly observations (bars) or discrete observations in time (dots). Data  
 69 are indicated as available if any variable is present for the given time. Sediment traps are not  
 70 hourly, but were collected over specific windows of time. January 1st of each year is marked  
 71 with a dotted line. Data collected from different parts of the Lake Peters catchment are shown  
 72 with different colors, in roughly the same order as they are discussed in Section 3. See Section  
 73 3 for a more detailed description of the data. Some data (Lake Peters TROLL casts and  
 74 bathymetry) are not represented in this figure.

## 75 2. Site description

76 Lake Peters (69.32°N, 145.05°W) lies at 853 meters above sea level (m a.s.l.) on the north side  
 77 of the Brooks Range, an east-west trending mountain range in Arctic Alaska. The Brooks Range  
 78 extends 1000 km, separating the Arctic coastal plain to the north from the Yukon Basin to the



79 south. The third tallest peak in the range, Mount Chamberlin (2712 m a.s.l.; Nolan and  
80 Deslauriers, 2016) lies 3 km east of Lake Peters.

81

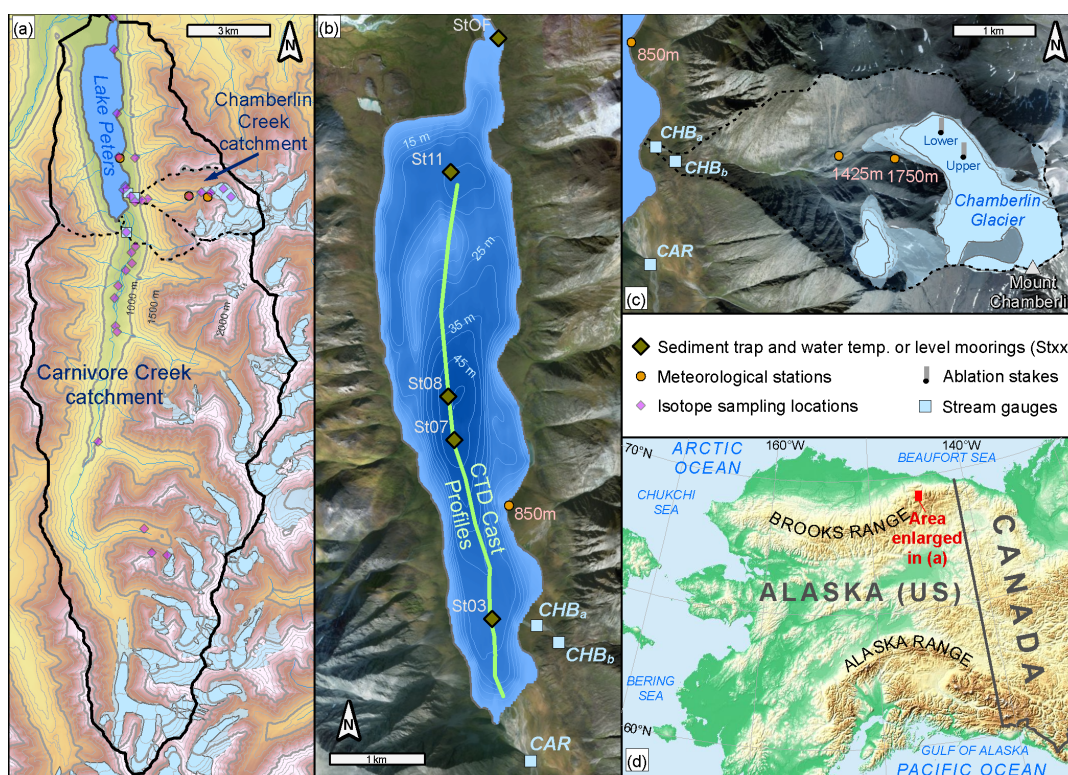
82 One of the largest glacier-fed lakes in Arctic Alaska, Lake Peters has a maximum water depth of  
83 52 m and an area of ~6.4 km<sup>2</sup>. The lake's catchment (171 km<sup>2</sup>) has 8% glacier coverage based  
84 on our aerial photography in 2016, and receives a majority of stream flow from Carnivore Creek,  
85 which has a 128 km<sup>2</sup> catchment with 10% glacier coverage (Fig. 2). The Carnivore catchment  
86 contains 6 glaciers exceeding 0.5 km<sup>2</sup> in area and numerous smaller glaciers, with a median  
87 elevation for all glaciers at 1910 m a.s.l. The largest glacier (3.5 km<sup>2</sup>; 1410 - 2430 m a.s.l.) is  
88 situated at the head of Carnivore Creek. Since the Little Ice Age, the largest few catchment  
89 glaciers have reduced in length by over 30%. Lake Peters' secondary inflow, Chamberlin Creek,  
90 has a 8 km<sup>2</sup> catchment that is 21% covered by Chamberlin Glacier (1.7 km<sup>2</sup>; 1600 - 2710 m  
91 a.s.l.) (Fig. 2). The lake drains to the north into Lake Schrader, whose outflow, the Kekiktuk  
92 River, discharges into the Sadlerochit River and ultimately the Arctic Ocean. Lake Peters and  
93 Lake Schrader, or "Neruokpuk Lakes", are ice covered from early October through mid-June or  
94 July, and often thermally stratify (Hobbie, 1961). The basin is north of the modern tree line in a  
95 region underlain by continuous permafrost, with a thin active layer where soils are rocky,  
96 excessively drained, strongly acidic, and have very thin surface organics. Bedrock within the  
97 basin is Devonian - Jurassic sedimentary to meta-sedimentary rocks primarily of the Neruopuk  
98 Formation (Reed, 1968).

99

100 Climate at Lake Peters is semi-continental, with temperatures more extreme than locations on  
101 the coastal plain. A short observational time series of weather from Lake Peters was initiated  
102 during the International Geophysical Year (Hobbie, 1962), and was summarized by March  
103 (2009). For the year between May 1, 2015 and April 30, 2016, weather stations installed in Lake  
104 Peters basin recorded an hourly averaged temperature of -9.8°C and a liquid precipitation total



105 of 166 mm. During this time period, average temperature was  $-29^{\circ}\text{C}$  in December and  $8.5^{\circ}\text{C}$  in  
106 July. Strong temperature inversions develop during the winter, with differences as large as  $15^{\circ}\text{C}$   
107 between 850 and 1425 m a.s.l.  
108



109  
110 Figure 2. (a) Lake Peters catchment (solid black boundary) and Carnivore and Chamberlin  
111 Creek sub-catchments (dashed boundaries) with terrestrial data sampling locations. (b) Lake  
112 Peters bathymetry and sampling locations. (c) Chamberlin Creek sub-catchment and  
113 Chamberlin Glacier. (d) Brooks Range setting in Alaska and study area location.

114  
115



## 116 3. Methods

### 117 3.1 Meteorological data

118 Three weather stations operated in the catchment from May 2015 through August 2018 along  
119 an elevational gradient (Fig. 3) (Kaufman et al., 2019c). The lowest elevation station was  
120 mounted on the roof of the cabin at the research station at 850 m a.s.l. near Lake Peters.  
121 Additional stations were installed on tripods at 1425 m a.s.l. inside the Little Ice Age moraine of  
122 Chamberlin Glacier, and the highest elevation station was at 1750 m a.s.l. at the crest of the left  
123 lateral moraine of Chamberlin Glacier (Fig. 3).

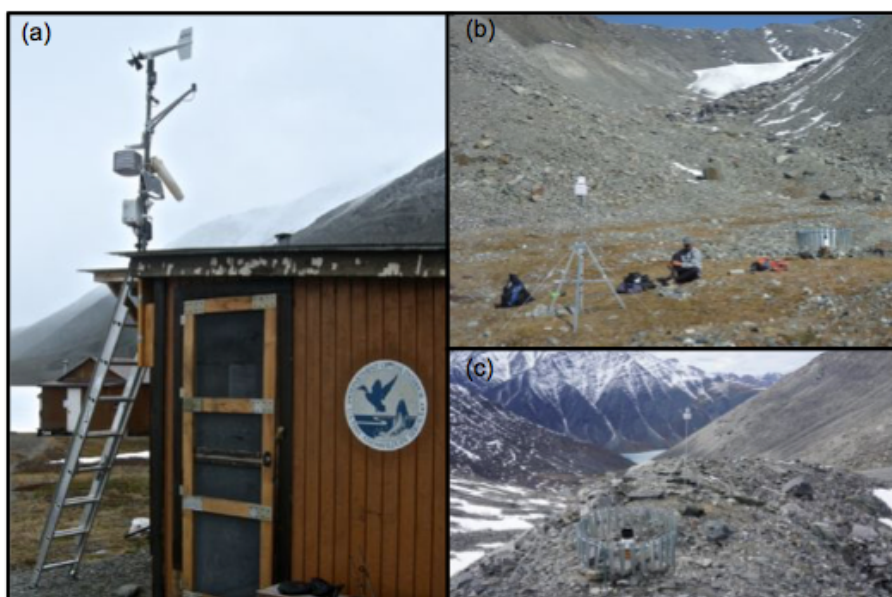
124

125 All three stations were equipped with air temperature and relative humidity sensors (Hobo Pro  
126 v2 Temp/RH sensors) and ground temperature sensors at 2 and 30 cm depth (Hobo Pro V2 2X  
127 w/ 6ft extension). The 850 and 1425 m a.s.l. stations were equipped with backup air  
128 temperature and relative humidity sensors (Hobo Pro v2 Temp/RH sensors). All temperature  
129 and relative humidity sensors were housed in Hobo Solar Radiation Shields. The 850 m a.s.l.  
130 station was additionally equipped with a barometer (Hobo Barometric Pressure Sensor S-BPB-  
131 CM50), an anemometer (Young Wind Monitor - 5103), and a pyranometer (Solar Radiation  
132 Sensor - S-LIB-M003). At all three stations, tipping bucket rain gauges (Hobo Rain gauge  
133 0.2mm w/pendant - RG3-M) were installed on the ground away from the stations and equipped  
134 with Alter-type windshields to reduce wind-related undercatch. Correlations between daily  
135 precipitation recorded at 850 m a.s.l. with daily precipitation recorded at 1425 and 1750 m a.s.l.  
136 indicate that trends are regionally coherent within the watershed with minimal (but expected)  
137 differences (Fig. 4).

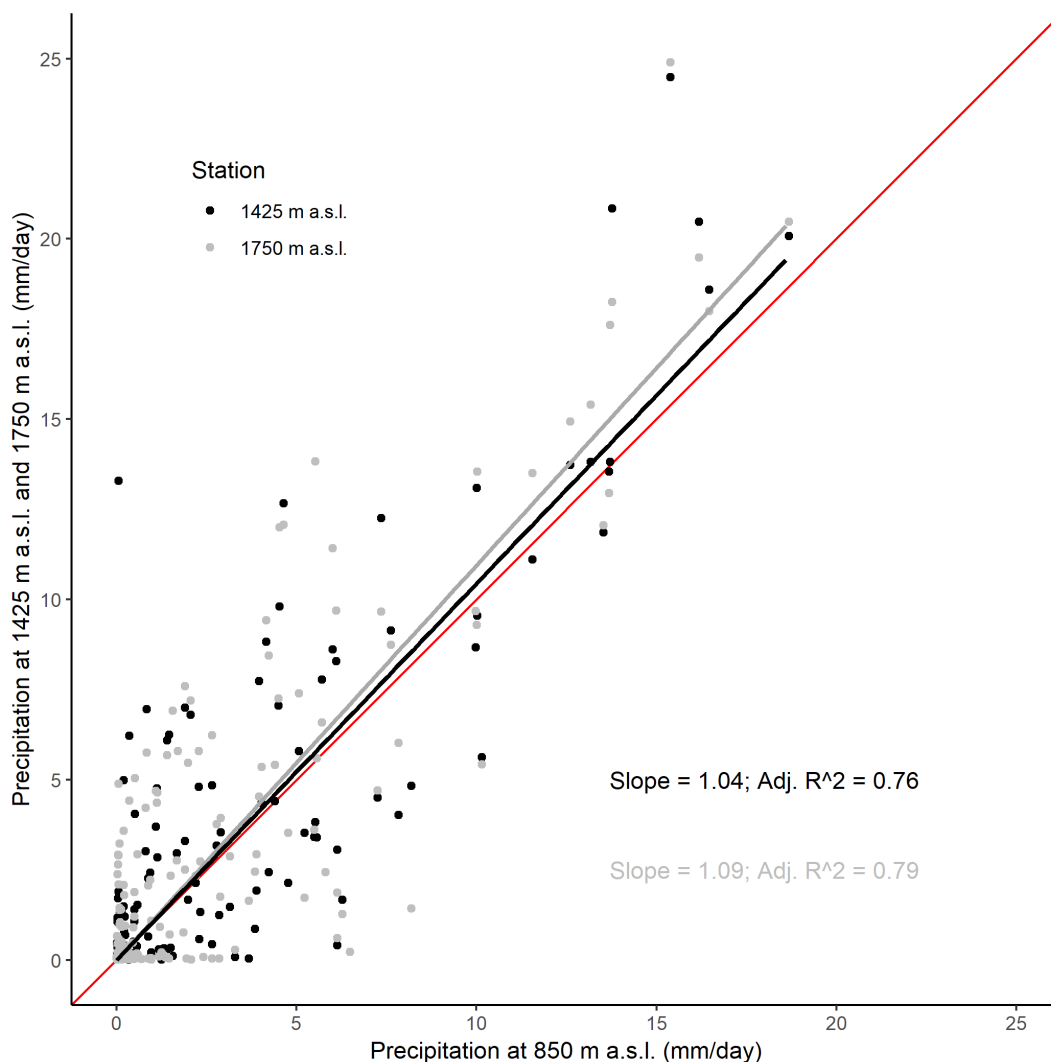
138



139 All three stations were generally continuously operational, though instrument failure caused  
140 gaps in the collection of some data from September 21, 2015 to April 19, 2016 at the 850 m  
141 a.s.l. station. Shorter instrument failures are documented for each sensor in the data files.  
142



143  
144 Figure 3. Weather stations at (a) 850, (b) 1425, and (c) 1750 m a.s.l. in the Lake Peters  
145 watershed.  
146  
147



148

149 Figure 4. Correlation of daily precipitation at 850 m a.s.l. with daily precipitation at 1425 and

150 1750 m a.s.l..

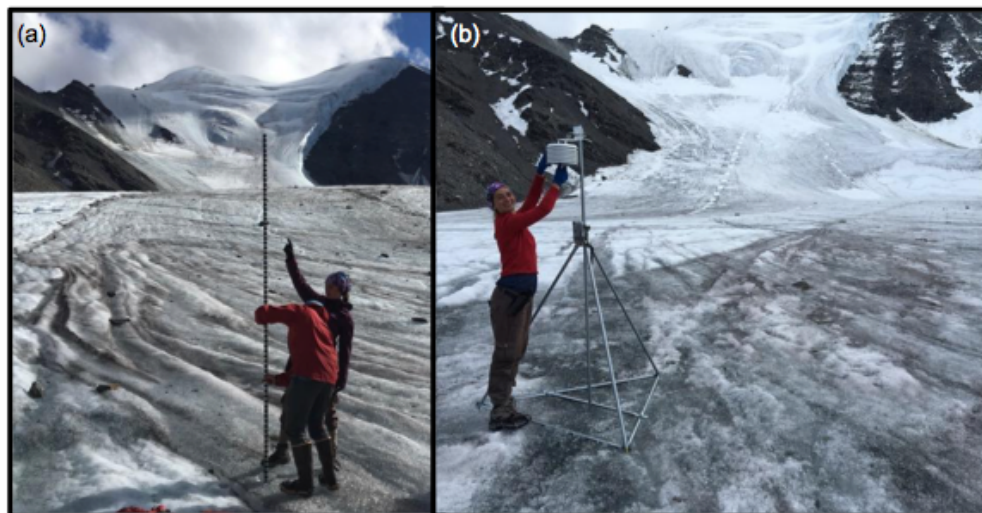
### 151 3.2 Glaciological data

152 The elevation of the surface of Chamberlain Glacier and its seasonal snow cover was observed

153 using ablation stakes and interval photography (Geck et al., 2019). Graduated stakes were



154 installed on April 27, 2016 at two sites along the lower part of the glacier: lower (69.29312°N,  
155 144.93814°W; 1772 m a.s.l.) and upper (69.29031°N, 144.93134°W; 1860 m a.s.l.). (Fig. 5a).  
156 Photographs captured exposed stakes height using Wingscapes Time-lapse Cameras (SKU:  
157 WCT-00122) set to automatically record every 6 hours. Ablation stake heights were observed  
158 on photographs (April 27, 2016 - August, 11, 2017) at a precision of 1 cm. Cameras were  
159 mounted on tripods constructed of electrical conduit (Fig. 5b). Air temperature sensors (Hobo  
160 Pro v2 Temp/RH sensors and/or Hobo Pendant) housed in Hobo Solar Radiation Shields  
161 recorded mean hourly temperatures 2 m above the snow surface at each site (Fig. 5b)  
162 (Kaufman et al., 2019f).



163  
164 Figure 5. Examples of (a) ablation stakes (lower site) and (b) weather stations (upper site)  
165 installed on Chamberlin Glacier.  
166

### 167 3.3 Fluvial data

168 Two hydrological stations were established in May 2015: one at Carnivore Creek (Schiefer et  
169 al., 2019b) and one at Chamberlin Creek (Schiefer et al., 2019c). At each station, an In-Situ



170 TROLL 9500 (TROLL) was deployed during the open-channel season to measure pressure,  
171 temperature, conductivity, and turbidity, and a Hobo Onset U20 Water Level logger was used  
172 for backup measurements of pressure and temperature. The instruments were attached to a  
173 cage constructed from aluminum tubing and chicken wire. A stage gage was installed at each of  
174 the hydrological stations, and water level and reach conditions were captured in hourly  
175 photographs by field cameras. Cages were installed in thalwegs of stable reaches and loaded  
176 with boulders to prevent movement (Fig. 6a). In August 2015 the instruments were detached  
177 and data were downloaded. In Carnivore Creek, the same procedure was completed for the  
178 2016, 2017, and 2018 field seasons (May-August), though data were not successfully retrieved  
179 from the TROLL in 2018. In Chamberlin Creek, the cage shifted several times during the 2015  
180 field season, and the instruments were consequently secured to channel-side bedrock for the  
181 2016 field season in an upstream pool near the alluvial fan apex (Fig. 6b). The instruments were  
182 ultimately carried downstream in the largest flood event of 2016, which peaked on July 16, and  
183 were subsequently secured to a large boulder for the 2017 field season, near the original 2015  
184 gauging station. No instruments were successfully deployed in Chamberlin Creek in 2018. In  
185 addition to these continuous datasets, discrete discharge (Q) and suspended sediment  
186 concentration measurements were taken using a hand-held Hach FH950 flow meter and a US  
187 DH-48 suspended sediment sampler, respectively.

188

189 Water pressure was corrected using barometric pressure measurements from the 850 m a.s.l.  
190 meteorological station and then converted to stage. Discrete field sampling of discharge was  
191 most frequent and spanned the greatest range in 2015. Discharge–stage regressions were used  
192 to construct continuous half-hourly discharge for the majority of the 2015 open-channel season  
193 in both Carnivore and Chamberlin Creeks (Fig. 7a-b). In Carnivore Creek, photographs of water  
194 level were imported to image viewing and analysis software to estimate 2.6 days of peak stage  
195 during a flood on August 3, 2015 (Fig. 7c) and its error margin. The regression used nine



196 photographs selected to capture maximal water-level variability, and stage was established  
197 using a point-to-point method to capture temporal variability. In Chamberlin Creek, linear  
198 relations between stage from the Hobo and TROLL instruments permitted compilation of a  
199 seamless discharge record for 2015 (Fig. 7d).

200

201 For the 2016 open-channel season, alternative methods were applied due to the lack of velocity  
202 data required to compute discharge, assuming consistent discharge-stage relations between  
203 seasons (Thurston, 2017). To formulate discharge for Carnivore Creek, stage was first  
204 regressed against cross-sectional area for both open-channel seasons separately (Fig. 7e).  
205 2016 stage was adjusted upward to be consistent with 2015 stage, accounting for the shift in  
206 instrument positioning between years. The 2015 stage-discharge relation could then be used to  
207 establish continuous 2016 season discharge from stage measured in 2016 (Fig. 7a). This  
208 method could not be applied to Chamberlin Creek because the TROLL and Hobo instruments  
209 were secured in different reaches between 2015 and 2016. Instead, 2015 discharge was  
210 regressed against cross-sectional area (Fig. 7f), and this relation was then used to construct  
211 discrete 'sampled' 2016 discharges from 2016 cross-sectional areas. Discharge-stage relations  
212 were used to formulate continuous discharge until a flood event beginning on June 20, 2016  
213 (Fig. 7g), at which point the instrumentation came loose and sensors failed. Several methods  
214 were used to construct stage and discharge for Chamberlin Creek following this flood (Fig. 7h-j).  
215 These methods included: photographs of river level from time-lapse cameras (46 days of  
216 discharge values); a regression of Chamberlin and Carnivore Creek discharges using all  
217 available data (3.6 days); a three-point stage-discharge rating curve, sampled downstream of  
218 the rating curve applied prior to the flood (8.8 days). When none of the aforementioned  
219 alternatives were possible, gaps were interpolated, amounting to a total of five gaps that range  
220 from 2 to 19 hours in length. The majority of the 2016 stage record (June 20 - August 5, 2016)  
221 was estimated for Chamberlin Creek from photographs of water level (Fig. 7h; Thurston, 2017).

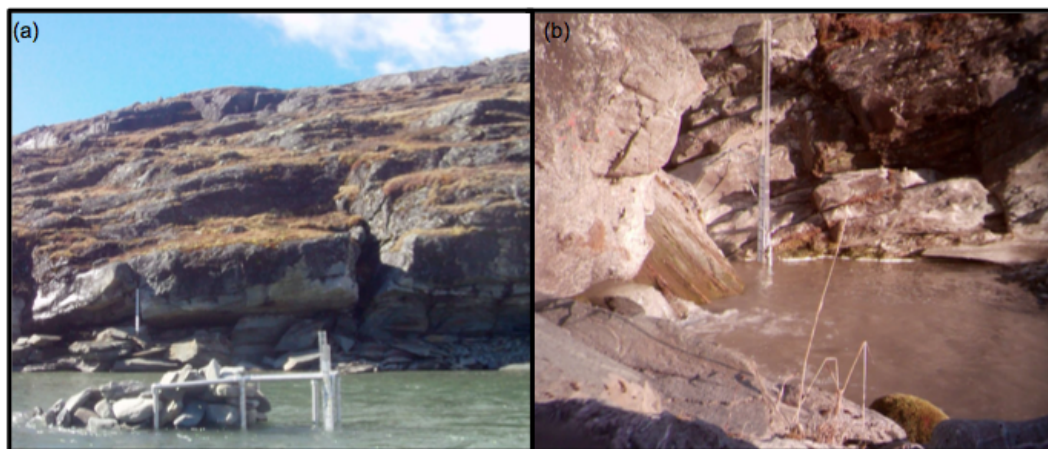


222 Water levels were measured using two reference points on a total of 13 photographs, then  
223 regressed separately against discharge. The first reference point was suitable for most  
224 discharges, but was not accurate after July 16, 2016 when water levels dropped low enough to  
225 expose a small bar. The second reference point was suitable for low discharges, but overtopped  
226 during high flows. Error was conservatively 10-20 image pixels, where 10 pixels equate to an  
227 approximately  $0.14 \text{ m}^3 \text{ s}^{-1}$  error margin in either direction from the average  $Q$  of  $0.72 \text{ m}^3 \text{ s}^{-1}$ . For  
228 the peak of this flood event on July 8, 2016 at 2:00, error is estimated to be 100 pixels in either  
229 direction because water level and control points were obscured (equating to a maximal error  
230 range of  $7.31 \text{ m}^3 \text{ s}^{-1}$  to  $49 \text{ m}^3 \text{ s}^{-1}$  for the peak  $Q$  of  $21 \text{ m}^3 \text{ s}^{-1}$ ). The Chamberlin station was  
231 ultimately re-established in a new location, and a new rating curve was used to reconstruct  $Q$   
232 from August 8, 2016 at 18:00 until August 17, 2016 at 13:00 (Fig. 7i). For Carnivore Creek data,  
233 the photographic method was favored over regression whenever photographs were available to  
234 keep the sub-catchment  $Q$  records independent. Considerable scatter between Carnivore and  
235 Chamberlin Creek  $Q$  records is attributed to hydrological differences between the sub-  
236 catchments (Fig. 7j). Summarized  $Q$  data alongside meteorological data at the 850 m a.s.l.  
237 station are shown in Fig. 8.

238

239 Few manual measurements of discharge or suspended sediment concentration were made in  
240 2017 and 2018. Stage-discharge rating curves developed from 2015 and 2016 data were used  
241 to convert continuous stage records to discharge for Carnivore Creek for 2017 and 2018, and  
242 Chamberlin Creek for 2017. Only minor adjustments were made, primarily to account for  
243 changes in instrumentation position relative to the channel bed. Instrumentation failure  
244 prevented development of a 2018 discharge record for Chamberlin Creek.

245

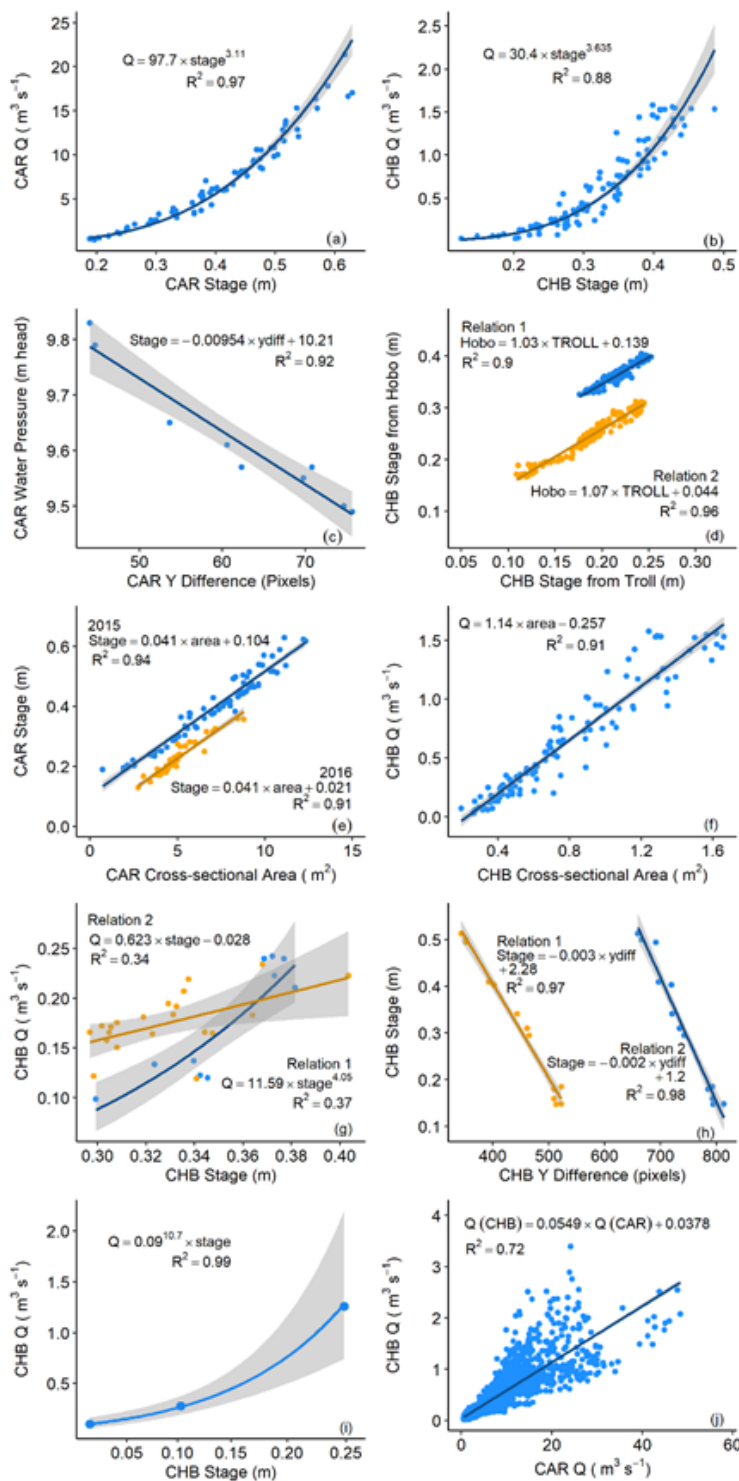


246

247 Figure 6. Stream stage gauges for (a) Carnivore and (b) Chamberlin Creeks in June 2016.

248 Instrumentation mounted in PVC tubing is obscured by stage gages.

249





251

252 Figure 7. Regression relations and associated confidence bands used to create continuous  
253 discharge (Q) time-series throughout the 2015-2018 open-channel seasons in Carnivore (CAR)  
254 and Chamberlin (CHB) Creeks. (a) Q – stage relation for CAR (2015); (b) Q – stage relation for  
255 CHB (2015); (c) water-pressure (from TROLL) – y difference (y-diff; shown on photographs)  
256 relation for CAR (2015); (d) relations of stage calculated from Hobo U20 water-pressure against  
257 stage calculated from TROLL 9500 water-pressure for CHB (both 2015); (e) stage – cross-  
258 sectional area linear relation for CAR (2015 and 2016); (f) Q – cross-sectional area linear  
259 relation for CHB (2015); (g) Q – stage (from Hobo) power relation for CHB (2016); (h) Stage – y  
260 difference (y-diff; shown on photographs) linear relations for CHB (both 2016); (i) Q – stage  
261 exponential relation for CHB (2016); and (j) Relation of Q in CHB against Q in CAR with a 2-  
262 hour lag (2015 and 2016). Refer to Thurston (2017) for additional information.

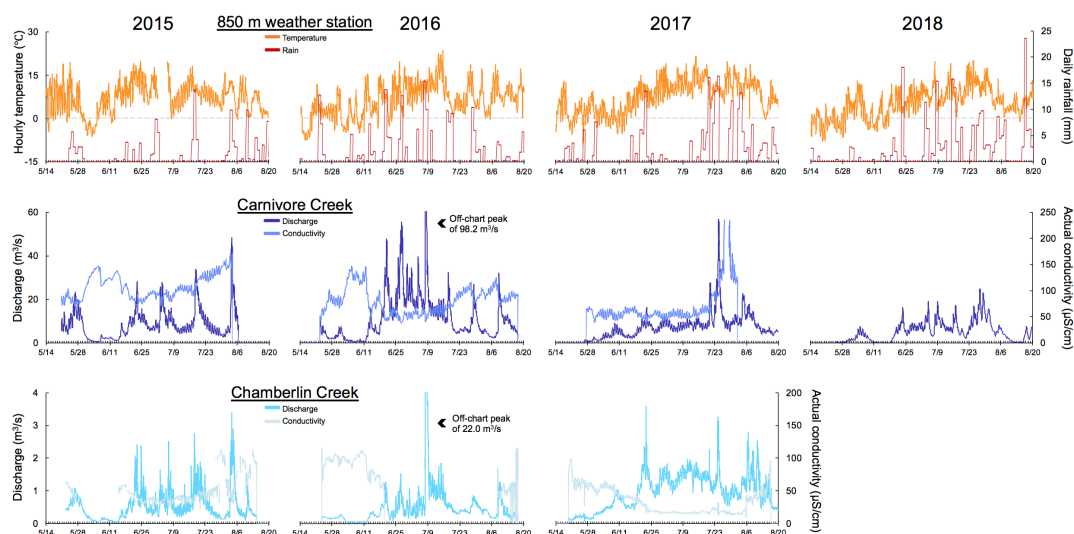
263

264

265

266

267



268

269 Figure 8. Time series of hourly air temperature and rainfall from the 850 m a.s.l. weather station  
270 at Lake Peters shown alongside conductivity and discharge for Carnivore and Chamberlin  
271 Creeks, 2015-2018.

272

## 273 3.4 Lacustrine data

### 274 3.4.1 Limnological data

275 Hourly water level measurements were taken using Hobo U20L Water Level loggers installed on  
276 anchored moorings near the water's surface at two locations in Lake Peters: one in its central  
277 basin and one near its outflow (Fortin et al., 2019a). Pressure data were corrected to water  
278 depth using barometric pressure measurements from the 850 m a.s.l. meteorological station.

279

280 Throughout the 2015 field season, a series of TROLL cast transects were taken to provide  
281 temperature, turbidity, and conductivity data at stations along a north-south transect throughout



282 Lake Peters (Fortin et al., 2019b). Pressure measurements from the TROLL were converted to  
283 water depth, providing vertical profiles for these data. These casts were performed at a varying  
284 number of stations on a total of 33 days over the course of the field season.

285

286 In 2015, 2016, and 2017, lake temperature and luminous flux data were collected at various  
287 water depths on anchored moorings throughout the lake (Fig. 2) (Kaufman et al., 2019b). The  
288 moorings were equipped with Hobo pendants and Hobo Water Temp Pro loggers at different  
289 water depths to monitor the thermal structure of the lake. Moorings located in the central basin  
290 of the lake were deployed from May 2015 until August 2016 (Station 7) and August 2015 until  
291 August 2017 (Station 8). A mooring in the distal basin (Station 11) was deployed from May 2015  
292 to August 2015, and a mooring in the proximal basin (Station 3) was deployed from May 2015  
293 until August 2015.

294

### 295 3.4.2 Sediment trap data

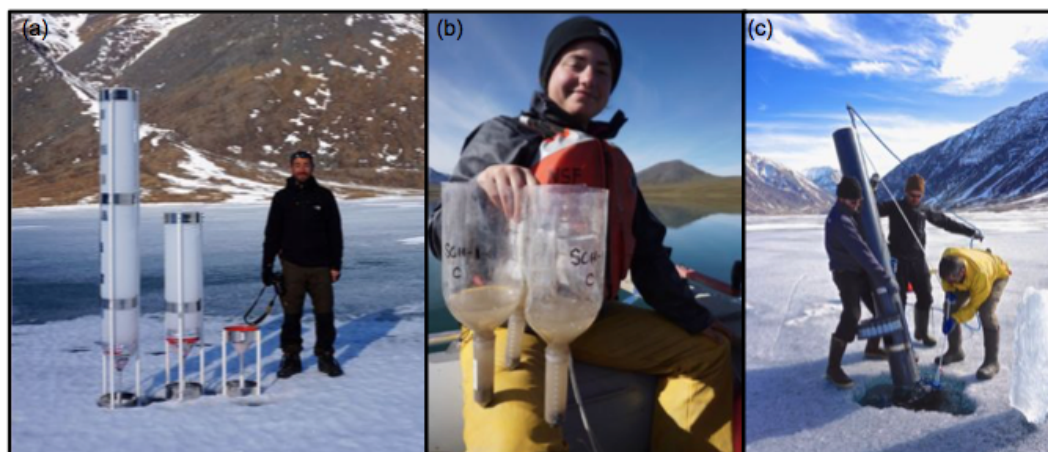
296 Throughout 2015-2017, sediment traps were deployed in Lake Peters to measure the rate of  
297 deposition and collect suspended sediments in the lakes (Kaufman et al., 2019d). In 2015, three  
298 pairs of static (i.e., non-automated) traps with different aspect ratios (different collection-tube  
299 heights but same collection-tube diameters) (Fig. 9a) were deployed from May-August at a  
300 central location of Lake Peters to determine the effect of these proportions on sediment  
301 collection efficiency. From May-August 2016 and again from August 2016 through August 2017  
302 one static trap was deployed in Lake Peters. This trap consisted of ordinary 2 L plastic bottles  
303 with the bottoms removed, a 50 ml centrifuge tube secured to its mouth, and inverted to funnel  
304 sediments into the tubes (Fig. 9b). Each trap comprised two or three replicate tubes/bottles  
305 deployed at different depths along an anchored mooring. In addition, an incrementing sediment



306 trap described by Muzzi and Eadie (2002) was deployed from May 2016 through August 2017,  
307 collecting sediments in 23 bottles rotating over daily to weekly increments (Fig. 9c).

308 For all sediment samples, dry sediment mass, daily flux, and annual flux were calculated. For  
309 several static trap samples, grain size data (mean, standard deviation, d50, d90, %sand, %silt,  
310 and %clay) were determined using a Coulter LS-320. Samples were pretreated with 30% H<sub>2</sub>O<sub>2</sub>  
311 and heated overnight at 50°C to remove organic material, and then treated with 10% Na<sub>2</sub>CO<sub>3</sub> for  
312 5 hours to remove biogenic silica. Pretreated samples were deflocculated by adding sodium  
313 hexametaphosphate and shaking for one hour before performing grain size analysis. Organic  
314 matter content for some samples was determined using loss on ignition analysis.

315



316

317 Figure 9. Examples of the types of sediment traps installed in Lake Peters: (a) installation of  
318 static traps ratio traps, (b) static traps upon retrieval, and (c) installation of an incrementing trap.

## 319 3.5 Spatial data

### 320 3.5.1 Bathymetry



321 Bathymetric data were collected using a Lowrance Elite-5 HDI Combo sonar depth recorder  
322 along several transects throughout Lake Peters in August 2015 (Schiefer et al., 2019a). These  
323 data were used to create a bathymetric map with ArcGIS 9.1.

324

### 325 3.5.2 High resolution photogrammetry

326 Airborne photogrammetric data were acquired two times in 2015 (April 23 and July 5), three  
327 times in 2016 (April 19, July 11, and August 5), and three times in 2017 (April 28, June 27, and  
328 September 3) (Nolan, 2019). These data were used to create digital elevation models (DEMs)  
329 with postings of 50-80 cm provided in NAD83(2011) NAVD88 Geoid 12B. When conditions  
330 permitted (April 23, 2015; July 5, 2015; April 19, 2016; April 28, 2017), the entire Carnivore  
331 Creek watershed was acquired. On all other dates, only the eastern side of the valley, where the  
332 catchment glaciers are located, was captured. These data were acquired using a Nikon DSLR  
333 attached to a survey grade GNSS on board a manned aircraft, providing photo-center position  
334 to 10 cm or better and thus eliminating the need for ground control. Accuracy within this steep  
335 mountain environment was found to exceed 20 cm horizontally and vertically (Nolan and  
336 Deslauriers, 2016), without use of ground control. Data acquisition methods are described in  
337 detail in Nolan et al. (2015). These DEMs were used to create difference DEMs that can be  
338 used to measure snowpack thickness throughout the entire watershed as well as glacier surface  
339 elevation change. The accuracy of these DEM-derived snow thickness measurements has  
340 previously been found to be comparable to those acquired using hand probes (Nolan et al.,  
341 2015). However, larger errors are expected in rugged mountain topography, as the 50 cm DEMs  
342 cannot resolve many small crenulations, likely causing some spatial biasing.



### 343 3.6 Geochemical data

344 A total of 187 water samples were collected from the Lake Peters catchment between 2015 and  
345 2018 and analyzed for isotopes of oxygen ( $\delta^{18}\text{O}$ ) and hydrogen ( $\delta\text{D}$ ) (‰VSMOW) (Kaufman et  
346 al., 2019a). These data, combined with conductivity measurements, were input to a hydrograph  
347 mixing model to estimate the relative contributions of various water sources to Carnivore and  
348 Chamberlin Creeks (Ellerbroek, 2018). Sampling intervals varied by location but were  
349 approximately every 2-6 days when a field team was present. In one 24-hour period in August  
350 2016, each creek was sampled every two hours using a Teledyne ISCO 3700 portable  
351 automatic water sampler (ISCO). These ISCO samples from Carnivore and Chamberlin Creeks  
352 were also analyzed for major cation and anion geochemistry analysis using a Dionex ICS-3000  
353 ion chromatograph with an analytical precision of  $\pm 5\%$  (Kaufman et al., 2019a). Water samples  
354 were also collected from three unnamed glaciated tributaries in the Carnivore Creek valley and  
355 three unnamed non-glacial streams that intermittently drain into Lake Peters. All samples were  
356 collected in 10 mL polyethylene bottles rinsed three times with sample water.

357

358 Winter precipitation samples were collected from multiple locations. Twenty-seven snowpack  
359 samples were collected with snow density measurements in April 2016 and May 2017 at a  
360 variety of depths from 21 snow cores along an elevational gradient. Samples of glacial melt,  
361 glacial ice, and snow drifts were collected over 2015 and 2016. All snow and ice samples were  
362 collected in airtight plastic bags and transferred into rinsed 10 mL polyethylene bottles after  
363 melting. Rain samples were collected sporadically after storm events from spill off from the roof  
364 of G. William Holmes research station and transferred into rinsed 10 mL polyethylene bottles.

365



366 Following each field season, water samples were processed using Wavelength-Scanned Cavity  
367 Ringdown Spectroscopy. Analytical precision is approximately 0.3‰ for  $\delta^{18}\text{O}$  and 0.8‰ for  $\delta\text{D}$   
368 (Los Gatos Research, 2018).

369

## 370 4. Data example: Tracing an event through the Lake 371 Peters glacier-river-lake system

372 To examine how precipitation works its way through the Lake Peters catchment system, and to  
373 depict a small subset of the available data, multiple datasets are shown for a precipitation event  
374 in the latter half of July 2015 (Figs. 10, 11). During this event, the 850 m a.s.l. meteorological  
375 station recorded a total rainfall of 22.4 mm between July 17-20 (Fig. 10a). In response,  
376 hydrological stations at both Carnivore and Chamberlin Creeks recorded an increase in  
377 discharge to Lake Peters, with Carnivore Creek discharge reaching far higher values due to its  
378 larger catchment (Fig. 2). Discharge then decreased over several weeks, long after the  
379 precipitation event concluded, with diurnal fluctuations illustrating the effect of glacial melt (Fig.  
380 10b). Turbidity increased in both creeks, coincident with the beginning of elevated discharge  
381 (Fig. 10c). The influx of water increased the water level of Lake Peters, which lagged, likely as a  
382 function of the total integration of new water as well as outflow into Lake Schrader (Fig. 10d).  
383 This event had several additional effects on the water of Lake Peters: Turbidity in Lake Peters  
384 increased during the event (Fig. 10e), the inflow of water caused a temporary drop in water  
385 temperatures closer to the lake surface (Fig. 10f), and the amount of luminous flux a few meters  
386 below the water's surface dropped (Fig. 10g). Isotopic values were also recorded from rainfall  
387 and creekwater at several moments during this event (Fig. 10h).

388



389 To quantify the spatial characteristics of the sediment pulse entering Lake Peters during this  
390 precipitation event, data from TROLL casts taken throughout the lake on multiple days before,  
391 during, and after the event were examined (Fig. 11). These data indicate that the spatial pattern  
392 of turbidity anomalies throughout Lake Peters is more complex than that captured at a single,  
393 proximal station shown in Fig. 10e.

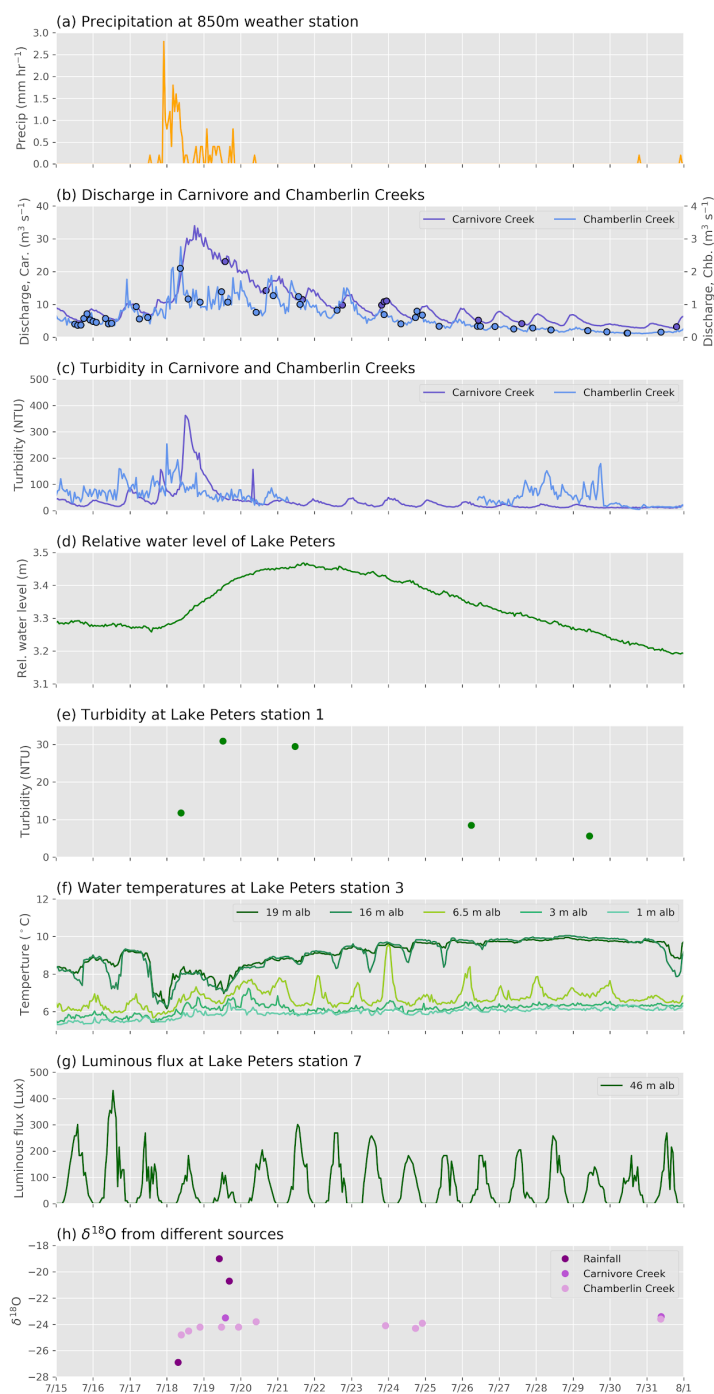
394

395 This multifaceted perspective of a precipitation event represents only a small fraction of the total  
396 data produced by this field effort, but illustrates both the interconnectedness of processes in the  
397 Lake Peters catchment and the potential for these datasets to further our understanding of  
398 Arctic weather-glacier-river-lake systems dynamics.

399

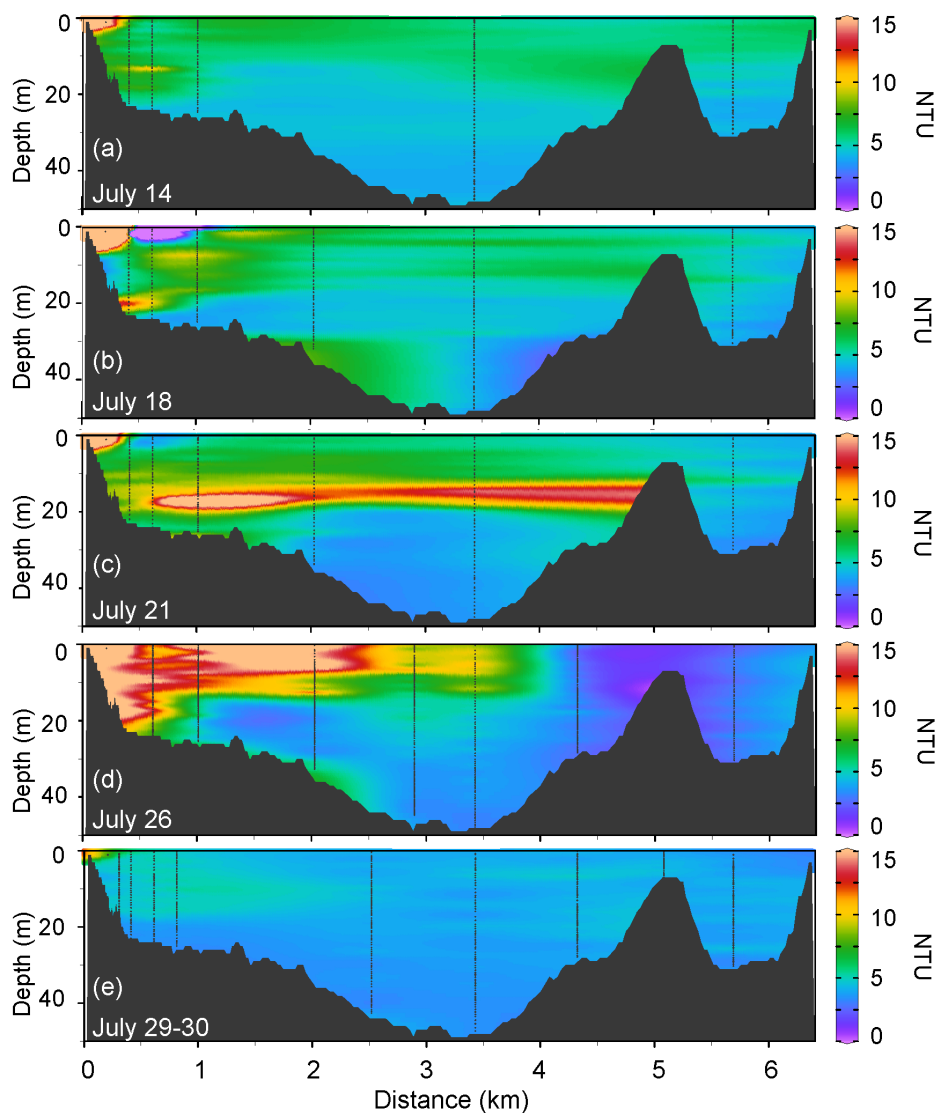


### Sample precipitation event in different datasets





401 Figure 10. An example of the observatory's data, tracing the effects of a precipitation event in  
402 July 2015. (a) Rainfall at the 850 m a.s.l. station; (b) Carnivore and Chamberlin Creek discharge  
403 and (c) turbidity; (d) Lake Peters relative water level, (e) maximum turbidity at Lake Peters  
404 station 1, (f) water temperatures at different heights above lake bottom (a.l.b.) at Lake Peters  
405 station 3, and (g) luminous flux at Lake Peters station 7; and (h)  $\delta^{18}\text{O}$  at different sites. To  
406 complement panel (e), a more detailed sample of turbidity data are shown in Fig. 11.



407

408 Figure 11. Turbidity in Lake Peters over the course of a precipitation event in July 2015; turbidity  
409 data are shown for (a) July 14, (b) July 18, (c) July 21, (d) July 26, and (e) composite data from  
410 July 29 and July 30. Black shading indicates lake bathymetry, and black dashed lines indicate  
411 locations of TROLL casts. The x-axis indicates north-south distance across the lake from the  
412 outflow of Carnivore Creek. Figure created using Ocean Data View (ODV) software.



## 413 5. Data availability

414 All DOI-referenced datasets described in this manuscript are archived at the National Science  
415 Foundation Arctic Data Center at the following overview webpage for the project:  
416 <https://arcticdata.io/catalog/view/urn:uuid:517b8679-20db-4c89-a29c-6410cbd08afe> (Kaufman  
417 et al., 2019e). Datasets are available for download (Table 1) as csv files (or tiffs for  
418 photogrammetry data) with accompanying metadata including an abstract, key words, methods,  
419 spatial and temporal coverage, and personnel information pertinent to each dataset.  
420



Dataset	Measured variables	Coordinates	Start date	End date	DOI
850 m a.s.l. meteorological station	barometric pressure (mbar), temperature (°C), relative humidity (%), solar radiation (W/m <sup>2</sup> ), wind speed (m/s), gust speed (m/s), wind direction (°), dew point (°C), ground temp at 2cm and 30cm (°C), precipitation (mm)	69.3046, -145.0342	15-05-13 21:00	18-08-22 15:00	<a href="https://doi.org/10.18739/A2V11VK4J">https://doi.org/10.18739/A2V11VK4J</a>
1425 m a.s.l. meteorological station	temperature (°C), relative humidity (%), ground temp at 2 cm and 30 cm (°C), precipitation (mm)	69.29094, -144.96983	15-05-24 16:00	18-05-26 14:00	<a href="https://doi.org/10.18739/A2V11VK4J">https://doi.org/10.18739/A2V11VK4J</a>
1750 m a.s.l. meteorological station	temperature (°C), relative humidity (%), ground temp at 2 cm and 30cm (°C), precipitation (mm)	69.29043, -144.95265	15-06-08 00:00	17-08-12 11:00	<a href="https://doi.org/10.18739/A2V11VK4J">https://doi.org/10.18739/A2V11VK4J</a>
Lower ablation stake	exposed stake height (cm)	69.29312, -144.93814	16-04-27 13:00	17-08-10 13:00	<a href="https://doi.org/10.18739/A2GQ6R21H">https://doi.org/10.18739/A2GQ6R21H</a>
Upper ablation stake	exposed stake height (cm)	69.29031, -144.93134	16-04-27 17:00	17-01-01 00:00	<a href="https://doi.org/10.18739/A2GQ6R21H">https://doi.org/10.18739/A2GQ6R21H</a>
Lower ablation stake meteorological station	temperature (°C)	69.29312, -144.93814	16-04-15 5:00	17-08-10 23:00	<a href="https://doi.org/10.18739/A2BZ6178M">https://doi.org/10.18739/A2BZ6178M</a>
Upper ablation stake meteorological station	temperature (°C), relative humidity (%)	69.29031, -144.93134	16-04-15 5:00	17-08-10 12:00	<a href="https://doi.org/10.18739/A2BZ6178M">https://doi.org/10.18739/A2BZ6178M</a>
Carnivore Creek manual data	discharge (m <sup>3</sup> /s), suspended sediment concentration (mol/L)	69.28028, -145.03051	15-05-16 17:02	17-08-14 16:00	<a href="https://doi.org/10.18739/A27659F58">https://doi.org/10.18739/A27659F58</a>
Chamberlin Creek manual data	discharge (m <sup>3</sup> /s), suspended sediment concentration (mol/L)	2015/2017: 69.2925, -145.0261 2016: 69.2910, -145.0203	15-05-16 17:44	17-08-14 16:50	<a href="https://doi.org/10.18739/A2MG7FV6Q">https://doi.org/10.18739/A2MG7FV6Q</a>
Carnivore Creek continuous data	conductivity (µm), temperature (°C), turbidity (NTU), pressure (m), discharge (m <sup>3</sup> /s)	69.28028, -145.03051	15-05-20 16:00	18-08-22 13:00	<a href="https://doi.org/10.18739/A27659F58">https://doi.org/10.18739/A27659F58</a>
Chamberlin Creek continuous data	conductivity (µm), temperature (°C), turbidity (NTU), pressure (m), discharge (m <sup>3</sup> /s)	2015/2017: 69.2925, -145.0261 2016: 69.2910, -145.0203	15-05-22 16:00	17-09-23 23:00	<a href="https://doi.org/10.18739/A2MG7FV6Q">https://doi.org/10.18739/A2MG7FV6Q</a>
Lake level	absolute (uncorrected) pressure (kPa), relative water level (m)	69.30993, -145.04644	15-05-20 16:00	17-08-06 10:00	<a href="https://doi.org/10.18739/A2KH0DZ5J">https://doi.org/10.18739/A2KH0DZ5J</a>
Station 3 mooring	temperature (°C) at 1, 3, 6.5, 16, and 19 meters above lake bottom	69.29336, -145.03813	15-05-28 12:00	15-08-01 8:00	<a href="https://doi.org/10.18739/A2FQ9Q52R">https://doi.org/10.18739/A2FQ9Q52R</a>
Station 7 mooring	temperature (°C) at 1, 3, 28, 44, and 46 meters above lake bottom; light intensity (Lux) at 28, 44, and 46 meters above lake bottom	69.30993, -145.04644	15-05-15 0:00	16-08-05 0:00	<a href="https://doi.org/10.18739/A2FQ9Q52R">https://doi.org/10.18739/A2FQ9Q52R</a>
Station 8 mooring	temperature (°C) at 1, 6, 11, 31, 41, and 48 meters above lake bottom; light intensity (Lux) at 48 meters above lake bottom	69.31496, -145.04766	15-08-09 12:00	17-08-06 9:00	<a href="https://doi.org/10.18739/A2FQ9Q52R">https://doi.org/10.18739/A2FQ9Q52R</a>
Station 11 mooring	temperature (°C) at 0.5, 3, 15, and 25 meters above lake bottom; light intensity (Lux) at 15 and 25 meters above lake bottom	69.33472, -145.04348	15-05-24 0:00	15-08-06 12:00	<a href="https://doi.org/10.18739/A2FQ9Q52R">https://doi.org/10.18739/A2FQ9Q52R</a>
CTD casts	temperature (°C), pressure-inferred depth (m), turbidity (NTU), conductivity (µm)	Various	15-05-21 15:34	15-08-12 11:24	<a href="https://doi.org/10.18739/A23J3912W">https://doi.org/10.18739/A23J3912W</a>
Sediment traps	mass (g), daily flux (mg/cm <sup>2</sup> /day), annual flux (g/cm <sup>2</sup> /year), organic matter content (%), grain size (µm)	Various	15-05-25	17-08-06	<a href="https://doi.org/10.18739/A2Q814S0S">https://doi.org/10.18739/A2Q814S0S</a>
Bathymetry	easting (UTM Zone 6N), northing (UTM Zone 6N), water depth (m)	Various	15-08	15-08	<a href="https://doi.org/10.18739/A2R785P0G">https://doi.org/10.18739/A2R785P0G</a>
Photogrammetry	high resolution DEM	Various	15-04-23	17-09-03	<a href="https://doi.org/10.18739/A28W3824W">https://doi.org/10.18739/A28W3824W</a>
Stable isotopes	δ <sup>18</sup> O (‰VSMOW), δD (‰VSMOW) d-excess (‰VSMOW)	Various	15-05-14 11:30	18-05-25 0:00	<a href="https://doi.org/10.18739/A2Z52KC8C">https://doi.org/10.18739/A2Z52KC8C</a>
Major cation and anion geochemistry	sulfate (ppm), calcium (ppm), magnesium (ppm), potassium (ppm), sodium (ppm), nitrate (ppm), chloride (ppm)	Various	16-08-12 18:00	16-08-18 20:00	<a href="https://doi.org/10.18739/A2Z52KC8C">https://doi.org/10.18739/A2Z52KC8C</a>

421

422 Table 1. Observational datasets generated by the Lake Peters observatory instrumentation and  
 423 archived at the NSF Arctic Data Center.

## 424 6. Final Remarks

425 The meteorological, glaciological, fluvial, and lacustrine datasets from Lake Peters and its  
 426 catchment presented in this manuscript offer a unique and valuable opportunity to study an  
 427 Arctic glacier-fed lake system. The observational data have contributed to our understanding of



428 individual events as well as intra- and inter-annual variability within this catchment. By making  
429 these data available, we hope to foster a more detailed understanding of the processes leading  
430 to sedimentation in Arctic lake catchments. Furthermore, these data may provide important  
431 context for interpretation of lake sediment records from this study region and elsewhere, as well  
432 as for hydrological and sedimentological modelling studies.

433

#### 434 **Supplement**

435 No supplements.

436

#### 437 **Author contributions**

438 N.P.M., D.S.K., E.S., D.F., J.G., M.G.L., and M.N. developed the observational design. E.B.,  
439 L.L.T., N.P.M., D.S.K., E.S., D.F., J.G., M.G.L., M.N., S.H.A., C.W.B., R.A.E., and C.C.R. led  
440 installation, development and/or curation of components of the observations. E.B., L.L.T.,  
441 N.P.M., D.S.K., E.S., J.G., M.P.E., C.W., and A.J.W. wrote the original manuscript. E.B., L.L.T.,  
442 N.P.M., E.S., D.F., S.H.A., R.A.E., M.P.E., C.W., and A.J.W. produced figures for the  
443 manuscript. E.B., D.F., and D.S.K. curated the datasets at the NSF Arctic Data Center. All  
444 authors provided minor edits to the text of the final manuscript.

445

#### 446 **Competing interests**

447 We declare no competing interests.

448

#### 449 **Acknowledgements**

450 Datasets from the Lake Peters watershed were collected with the help of numerous field  
451 assistants, including Zak Armacost, Mindy Bell, Ashley Brown, Anne Gädeke, Jeff Gutierrez,  
452 Rebecca Harris, Stacy Kish, Lisa Koeneman, Anna Liljedahl, Maryann Ramos, Doug Steen, and  
453 Ethan Yackulic. Sedimentary grain size data were processed with assistance from Daniel



454 Cameron and Katherine Whitacre. Water isotope analyses were performed with assistance from  
455 Jamie Brown at NAU's Colorado Plateau Stable Isotope Facility, and major cation and anion  
456 analyses were performed by Tom Douglas of the U.S. Army Cold Regions Research and  
457 Engineering Laboratory. We thank the U.S. Fish and Wildlife Service - Arctic National Wildlife  
458 Refuge for use of the G. William Holmes research station and for permitting our research; Polar  
459 Field Services, Inc./CH2MHill for support and outfitting while in the field; Dirk Nickisch and  
460 Danielle Tirrell of Coyote Air for safely flying our field teams to and from Lake Peters;  
461 LacCore/CSDCO for assistance with processing and archiving of sedimentary sequences from  
462 Lake Peters; and PolarTREC for a productive partnership that contributed greatly to the broader  
463 impacts of this project. This project was funded by NSF-1418000.

464

465

466

467

468

469

470

471

472

473

474

475

476

477

478

479



480 **References**

481

482 Benson, C.W.: 16,000 Years of Paleoenvironmental Change from the Lake Peters-Schrader  
483 Area, Northeastern Brooks Range, Alaska, M.S. thesis, Northern Arizona University, Flagstaff,  
484 Arizona, USA, AAT 10812107, 2018.

485

486 Benson, C.W., Kaufman, D.S., McKay, N.P., Schiefer, E., and Fortin, D.: A 16,000 year-long  
487 sedimentary sequence from Lake Peters and Schrader (Nerukpuk Lakes), northeastern Brooks  
488 Range, Alaska, Quaternary Res., in review.

489

490 Ellerbroek, R.A.: Three Component Hydrograph Separation for the Glaciated Lake Peters  
491 Catchment, Arctic Alaska, M.S. thesis, School of Earth and Sustainability, Northern Arizona  
492 University, Flagstaff, Arizona, USA, ProQuest ID 2112380481, 2018.

493

494 Fortin, D., Kaufman, D.S., Schiefer, E., Thurston, L.L., Geck, J., Loso, M.G., McKay, N.P.,  
495 Liljedahl, A., and Broadman, E.: Lake Peters water level, Arctic National Wildlife Refuge,  
496 Alaska, 2015-2017, doi:10.18739/a2kh0dz5j, 2019a.

497

498 Fortin, D., Schiefer, E., Thurston, L.L., Kaufman, D.S., Geck, J., Loso, M.G., McKay, N.P.,  
499 Liljedahl, A., and Broadman, E.: CTD casts (conductivity, temperature, depth) in Lake Peters,  
500 Arctic National Wildlife Refuge, Alaska, 2015, doi:10.18739/a23j3912w, 2019b.

501

502 Geck, J., Loso, M.G., Schiefer, E., Thurston, L.L., McKay, N.P., Kaufman, D.S., Fortin, D.,  
503 Liljedahl, A., and Broadman, E.: Ablation stake data from Chamberlin Glacier, Arctic National  
504 Wildlife Refuge, Alaska, 2016-2017, doi:10.18739/a2gq6r21h, 2019.

505



506 Hobbie, J.E.: Summer temperatures in Lake Schrader, Alaska, *Limnol. Oceanogr.*, 6, 326-329,  
507 <https://doi.org/10.4319/lo.1961.6.3.0326>, 1961.  
508  
509 Hobbie, J.E.: Limnological cycles and primary productivity of two lakes in the Alaskan Arctic,  
510 Ph.D. thesis, Department of Zoology, Indiana University, Bloomington, Indiana, USA, 1962.  
511  
512 Kaufman, D.S., Ellerbroek, R.A., Fortin, D., Schiefer, E., Thurston, L.L., Geck, J., Loso, M.G.,  
513 McKay, N.P., Liljedahl, A., and Broadman, E.: Geochemical and stable isotope composition data  
514 from precipitation, runoff, snow and ice collected in Lake Peters watershed, Arctic Wildlife  
515 Refuge, Alaska, 2015-2018, doi:10.18739/a2zs2kc8c, 2019a.  
516  
517 Kaufman, D.S., Fortin, D., Schiefer, E., Thurston, L.L., Geck, J., Loso, M.G., McKay, N.P.,  
518 Liljedahl, A., and Broadman, E.: Lake Peters water temperature and luminous flux, Alaska,  
519 2015-2017, doi:10.18739/a2fq9q52r, 2019b.  
520  
521 Kaufman, D.S., Fortin, D., Schiefer, E., Thurston, L.L., Geck, J., Loso, M.G., McKay, N.P.,  
522 Liljedahl, A., and Broadman, E.: Meteorological data from the Lake Peters watershed, Arctic  
523 National Wildlife Refuge, Alaska, 2015-2018, doi:10.18739/a2v11vk4j, 2019c.  
524  
525 Kaufman, D.S., Fortin, D., Schiefer, E., Thurston, L.L., Geck, J., Loso, M.G., McKay, N.P.,  
526 Liljedahl, A., and Broadman, E.: Sediment trap data from Lake Peters and Lake Schrader, Arctic  
527 National Wildlife Refuge, Alaska, 2015-2017, doi:10.18739/a2q814s0s, 2019d.  
528  
529 Kaufman, D.S., Fortin, D., Schiefer, E., Thurston, L.L., Geck, J., Loso, M.G., McKay, N.P.,  
530 Liljedahl, A., Broadman, E., Benson, C. W., Nolan, M., and Ellerbroek, R. A., Collaborative  
531 research: Developing a System Model of Arctic Glacial Lake Sedimentation for Investigating



532 Past and Future Climate Change, Arctic Data Center,  
533 <https://arcticdata.io/catalog/view/urn:uuid:517b8679-20db-4c89-a29c-6410cbd08afe>, 2019e.  
534  
535 Kaufman, D.S., Geck, J., Loso, M.G., Schiefer, E., Thurston, L.L., McKay, N.P., Fortin, D.,  
536 Liljedahl, A., and Broadman, E.: Meteorological data from Chamberlin Glacier, Arctic National  
537 Wildlife Refuge, Alaska, 2016-2017, doi:10.18739/a2bz6178m, 2019f.  
538  
539 March, J.R.: Synoptic climatology of the eastern Brooks Range, Alaska: a data legacy of the  
540 International Geophysical Year, M.S. thesis, Department of Atmospheric Science, University of  
541 Alaska, Fairbanks, Alaska, USA, 2009.  
542  
543 Muzzi, R.W. and Eadie, B.J.: The design and performance of a sequencing sediment trap for  
544 lake research. *Mar. Technol. Soc. J.*, 36, 2-28, <https://doi.org/10.4031/002533202787914025>,  
545 2002.  
546  
547 Nolan, M., Larsen, C., and Sturm, M.: Mapping snow depth from manned aircraft on landscape  
548 scales at centimeter resolution using structure from motion photogrammetry, *The Cryosphere*,  
549 9, 1445-1463, <https://doi.org/10.5194/tc-9-1445-2015>, 2015.  
550  
551 Nolan, M.: High resolution photogrammetric data of Chamberlin Glacier and the Lake Peters  
552 watershed, Alaska, 2015-2017, doi:10.18739/a28w3824w, 2019.  
553  
554 Nolan, M. and DesLauriers, K.: Which are the highest peaks in the US Arctic? Fodar settles the  
555 debate, *The Cryosphere*, 10, 1245-1257, <https://doi.org/10.5194/tc-10-1245-2016>, 2016.  
556



- 557 Reed, B.: Geology of the Lake Peters area northeastern Brooks Range, Alaska. U.S. Geol.  
558 Surv. Bulletin 1236, 132 pp., 1968.  
559
- 560 Schiefer, E., McKay, N.P., Kaufman, D.S., Fortin, D., Geck, J., Loso, M.G., Liljedahl, A., and  
561 Broadman, E.: Bathymetric map of Lake Peters, Alaska, 2015, doi:10.18739/a2r785p0g, 2019a.  
562
- 563 Schiefer, E., Thurston, L.L., Kaufman, D.S., Geck, J., Loso, M.G., McKay, N.P., Fortin, D.,  
564 Liljedahl, A., and Broadman, E.: Carnivore Creek discharge and suspended sediment  
565 concentration, Alaska, 2015-2018, doi:10.18739/a27659f58, 2019b.  
566
- 567 Schiefer, E., Thurston, L.L., McKay, N.P., Kaufman, D.S., Fortin, D., Geck, J., Loso, M.G.,  
568 Liljedahl, A., and Broadman, E.: Chamberlin Creek discharge and suspended sediment  
569 concentration, Alaska, 2015-2017, doi:10.18739/a2mg7fv6q, 2019c.  
570
- 571 Thurston, L.L.: Modeling Fine-grained Fluxes for Estimating Sediment Yields and Understanding  
572 Hydroclimatic and Geomorphic Processes at Lake Peters, Brooks Range, Arctic Alaska, M.S.  
573 thesis, Northern Arizona University, Flagstaff, Arizona, USA, ProQuest ID 2025947690, 2017.